The LUMO of **4** shown in **5** is also Tl–FeL_3 bonding. It is of

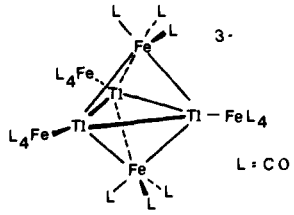

4

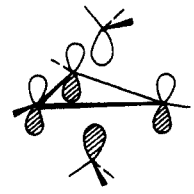

5

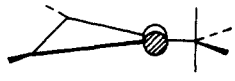

6

7

a_2'' symmetry and lies at much higher energy that the other eight valence molecular orbitals (the HOMO–LUMO gap was computed to be 2.3 eV).[19]

What, then, is the electronic basis for forming a dimeric structure from **4** and, furthermore, in what region of the dimer does the electron deficiency reside; i.e., is it retained in the $Tl_3(\mu_3\text{-}Fe(CO)_3)_2$ fragment or is it associated with the $Tl_2(\mu_2\text{-}Fe(CO)_4)_2$ portion of the molecule? In order for dimerization to occur, one of the terminal FeL_4 units of **4** must pseudorotate so that the thallium is coordinated at an equatorial rather than an axial position, but the electronic details of this new configuration are not significantly different from those for **4**. There are two ways to view formation of the dimer. Along with the dative, two-electron Tl–FeL_4 bond, one has an empty p orbital on Tl, **6**, and a filled d orbital on the FeL_4, **7**. First, the dative Tl–FeL_4 bond along with **6** and **7** can combine in the dimer to yield four occupied two-center, two-electron Tl–Fe bonds. Alternatively, one could construct electron deficiency in this region of the molecule by using these four orbitals to form two three-center two-electron bonds. The extra four electrons would be placed in the two molecular orbitals of the dimer corresponding to symmetry-adapted combinations of **5**. Our computations suggest that there are four two-center two-electron bonds in the Tl-bridging FeL_4 region. The two LUMO's of the dimer are clearly identified as combinations of **5**. The electron deficiency, therefore, appears to be in the Tl–FeL_3 portion of the molecule.

Acknowledgment. The Robert A. Welch Foundation (T.A.A. and K.H.W.), the donors of the Petroleum Research Fund, administered by the American Chemical Society (T.A.A. and K. H.W.), the Sloan Foundation (T.A.A.), the Department of Energy and the National Science Foundation (CHE 8421217) are gratefully acknowledged for their support of this work. Associated Western Universities provided support for K.H.W. to collaborate with Los Alamos National Laboratory on the structural investigation. We also thank Professor J. K. Burdett for enlightening conversations.

Registry No. 1, 104337-74-8; **3**, 104337-76-0; **4**, 104351-50-0; $Fe(CO)_5$, 13463-40-6; Tl, 7440-28-0; Fe, 7439-89-6.

Supplementary Material Available: Tables of bond distances and angles, crystallographic data collection parameters, atom coordinates, and isotropic and anisotropic thermal parameters and an ORTEP diagram of the full anion showing all carbonyl ligands (10 pages); structure factor tables (11 pages). Ordering information is given on any current masthead page.

(18) The FeL_4 groups in **4** are assumed to have C_{3v} symmetry; thus, the maximum symmetry of 4 is C_{3v}. The C_{3v} FeL_4 group is, however, a concial fragment, thus, the apparent summetry is D_{3h} and we have used symmetry labels which conform to this.

(19) the $L_3Fe\text{--}FeL_3$ bonding counterpart of **4** (a_1' symmetry) is filled; thus one might propose that there should be a single bond between the two FeL_3 groups; however, the total overlap population between these two iron atoms is only 0.041 and the long distance argues strongly against this hypothesis.

EXAFS Studies of the B_2 Subunit of the Ribonucleotide Reductase from *E. coli*

Robert C. Scarrow, Michael J. Maroney,† Sharon M. Palmer,† and Lawrence Que, Jr.*

Department of Chemistry, University of Minnesota Minneapolis, Minnesota 55455

Scott P. Salowe and JoAnne Stubbe

Department of Biochemistry, College of Agriculture and Life Sciences, University of Wisconsin—Madison Madison, Wisconsin 53706

Received May 12, 1986

Ribonucleotide reductases catalyze the conversion of ribonucleotides to deoxyribonucleotides and thus play a key role in regulating DNA biosynthesis.[1] The enzyme from *E. coli* consists of two subunits[2] designated B_1 (M_r = 170000)[3] and B_2 (M_r = 87000).[3] B_1 contains the substrate binding sites and the thiols required for substrate reduction,[4] while B_2 possesses a binuclear iron site and the tyrosine radical essential for activity.[5] The binuclear iron site has been probed by a variety of physical techniques. The site exhibits strong antiferromagnetic coupling ($J = -108$ cm^{-1}),[6] large Mössbauer quadrupole splittings,[7] and Raman vibrations characteristic of an Fe–O–Fe bridging unit.[8] These properties bear a striking resemblance to those of the binuclear iron cluster in methemerythrins.[9,10] We report here an iron K-edge EXAFS study of the B_2 subunit of ribonucleotide reductase from *E. coli* (B_2).

Subunit B_2 was isolated from *E. coli* strain N6405/pSPS2, a heat-inducible overproducer,[11] while methemerythrin azide (metHrN_3) was obtained from *Phascolopsis gouldii*.[12] X-ray absorption spectra were obtained at the Cornell High Energy Synchrotron Source on the C2 beam line using fluorescence detection for the proteins at 77 K;[13] the specific activities and the UV–visible spectra of the protein samples were unchanged after data collection. Spectra for model compounds were obtained in transmission mode. EXAFS (χ) was extracted from the X-ray absorption spectrum by standard methods.[14] Curve fitting employed theoretical amplitude and phase functions.[15]

EXAFS spectra obtained for native B_2 and its radical-free (hydroxyurea-treated[16]) form are similar. The spectrum for native

† Present address: Department of Chemistry, University of Massachusetts, Amherst, MA 01003.

(1) Lammers, M.; Follman, H. *Struct. Bonding (Berlin)* **1983**, *54*, 27–91. Reichard, P.; Ehrenberg, A. *Science (Washington, D.C.)* **1983**, *221*, 514–519. Thelander, L.; Reichard, P. *Annu. Rev. Biochem.* **1979**, *48*, 133–158.
(2) Thelander, L. *J. Biol. Chem.* **1973**, *248*, 4591–4601.
(3) Carlson, J.; Fuchs, J. A.; Messing, J. *Proc. Natl. Acad. Sci. U.S.A.* **1984**, *81*, 4294–4297.
(4) Thelander, L. *J. Biol. Chem.* **1974**, *249*, 4858–4862.
(5) Sjöberg, B.-M.; Reichard, P.; Graslund, A.; Ehrenberg, A. *J. Biol. Chem.* **1978**, *253*, 6863–6865. Sjöberg, B.-M.; Graslund, A. *Adv. Inorg. Biochem.* **1983**, *5*, 87–110.
(6) Petersson, L.; Graslund, A.; Ehrenberg, A.; Sjöberg, B.-M.; Reichard, P. *J. Biol. Chem.* **1980**, *255*, 6706–6712.
(7) Atkin, C. L.; Thelander, L.; Reichard, P.; Lang, G. *J. Biol. Chem.* **1973**, *248*, 7464–7472.
(8) Sjöberg, B.-M.; Loehr, T. M.; Sanders-Loehr, J. *Biochemistry* **1982**, *21*, 96–102.
(9) Stenkamp, R. E.; Sieker, L. C.; Jensen, L. H. *J. Am. Chem. Soc.* **1984**, *106*, 618–622.
(10) Klotz, I. M.; Kurtz, D. M., Jr. *Acc. Chem. Res.* **1984**, *17*, 16–22. Wilkins, R. G.; Harrington, P. C. *Adv. Inorg. Biochem.* **1983**, *5*, 51–85.
(11) Salowe, S. P.; Stubbe, J. *J. Bacteriol.* **1986**, *165*, 363–366.
(12) Elam, W. T.; Stern, E. A.; McCallum, J. D.; Sanders-Loehr, J. *J. Am. Chem. Soc.* **1982**, *104*, 6369–6373.
(13) Roe, A. L.; Schneider, D. J.; Mayer, R. J.; Pyrz, J. W.; Widom, J.; Que, L., Jr. *J. Am. Chem. Soc.* **1984**, *106*, 1676–1681.
(14) Scott, R. A. *Methods Enzymol.* **1985**, *117*, 414–459.
(15) Teo, B. K.; Lee, P. A. *J. Am. Chem. Soc.* **1979**, *101*, 2815–2832. Teo, B. K.; Antonio, M. R.; Averill, B. A. *J. Am. Chem. Soc.* **1983**, *105*, 3751–3762.
(16) Kjoller-Larsen, I.; Sjöberg, B.-M.; Thelander, L. *Eur. J. Biochem.* **1982**, *125*, 75–81.

0002-7863/86/1508-6832$01.50/0

Table I. Parameters[a] from Least-Squares Fitting of $k^3\chi$ EXAFS Data

shell	1A		1B		2A		2B		3	
composition	1O		5(O,N)		n C,σ^2 = 40[b]		1Fe		n C,σ^2 = 60[c]	
A_i	0.44[b]		0.44[b]		0.44[b]		0.77[d]		0.8[c]	
ΔE_i	9.0[e]		9.0[e]		0.0[b]		−5.0[d]		−22.0[c]	
sample	r	σ^2[f]	r	σ^2	r	n	r	σ^2	r	n
B_2, no. 1	1.79	−36	2.06	6	3.04	3.5	3.22	9	4.30	4
B_2, no. 2	1.81	−35	2.07	7	3.01	2.2	3.21	33	4.30	5
B_2, no. 1 + no. 2	1.79	−32	2.06	11	3.03	3.1	3.22	21	4.30	4
B_2(HU)[g]	1.78	−25	2.06	30	2.99	5.7	3.19	17	4.30	4
metHrN_3	1.80	−19	2.13	10	3.05	4.2	3.19	27	4.33	5
$(HBpz_3Fe)_2O(OAc)_2$	1.79	0	2.12	21	3.07	3.8	3.16	35	4.34	5

[a] Units for r and σ^2 in Å and 10^{-4} Å^2, respectively. After initial estimates of r and σ(or n) were obtained from analysis of Fourier-filtered data, values for all shells were simultaneously refined on unfiltered data from k = 4.0–14.3 Å^{-1}. [b] Determined by using compound I. [c] Determined by using compounds II and V. [d] Determined by using the difference spectrum between compounds II(r_{Fe-Fe} = 3.15 Å) and V(r_{Fe-Fe} = 3.44 Å). The difference spectrum was used to minimize interference from shell 2A and other second shell light atom scatterers. [e] Determined by using compounds I–V. [f] Values for σ^2 are sensitive to inaccuracies in amplitude functions;[14] hence only relative values are significant. [g] B_2(HU) is the hydroxyurea-treated sample of B_2.

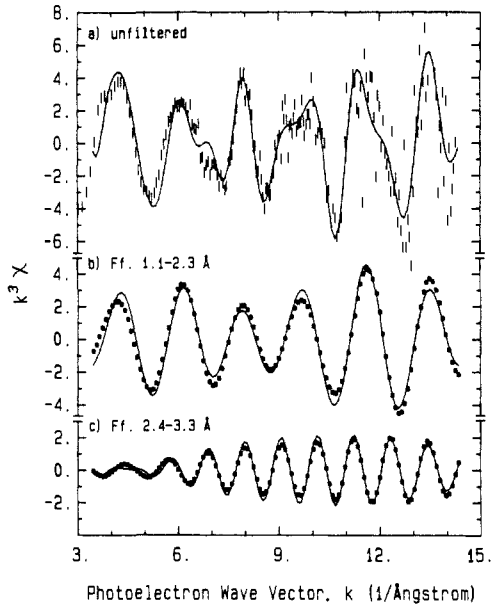

Figure 1. EXAFS spectra of native ribonucleotide reductase B_2 subunit (sum of samples 1 and 2) in k space (dashes or filled circles) together with spectra calculated by using parameters in Table I (lines). Shown are (a) the raw data, (b) the first shell, obtained by a back-transform of Figure 2 from r = 1.1–2.3 Å, and (c) the second shell, back-transformed from r = 2.4–3.3 Å. Protein concentration was 2.8 mM in 50 mM Tris acetate buffer pH 7.6 containing 0.1 mM Na_2EDTA and 20% glycerol.

B_2 is shown in k space in Figure 1 and in r space in Figure 2. The first shell consists of the two peaks below 2 Å in Figure 2; these features are attributed to partially resolved contributions from one short Fe–O bond (shell 1A) and longer Fe–X bonds (shell 1B). The difference in bond lengths causes the interference observed in the Fourier-filtered EXAFS (Figure 1B). The second shell (at ca. 3 Å in Figure 2) is dominated by an Fe–Fe component. The third shell (at ca. 4 Å in Figure 2) is attributed to low Z scatterers.

Curve fitting of the $k^3\chi$ data (as in Figure 1a) allowed determination of Fe–X distances (r) and either the disorder factor (σ^2) or, for carbon, the apparent number of atoms (n) per shell.[15] EXAFS of synthetic complexes were analyzed to determine amplitude reduction (A) and edge shift (ΔE) values for the Fe–X scatterer pairs as shown in Table I. The complexes used were $Fe(acac)_3$ (I)[17,18] and complexes with structures akin to the active site of metHrN_3, namely, $[(HBpz_3Fe)_2O(OAc)_2]$ (II)[19]

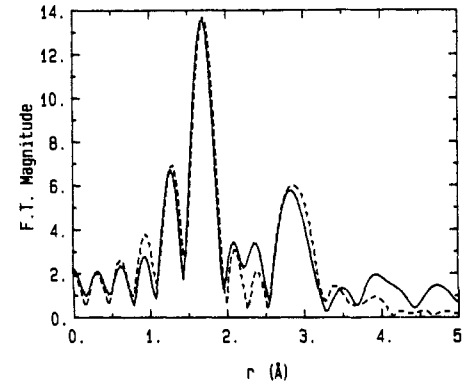

Figure 2. Fourier transform of native ribonucleotide reductase B_2 EXAFS spectra shown in Figure 1a [(—) experimental; (---) calculated] from k = 3.5–14.3 Å^{-1} with a 5% window.

$[(HBpz_3Fe)_2O(O_2P(OPh)_2)_2]$ (III)[20] $[(tacnFe)_2O(OAc)_2]I_2$ (IV),[21] and $[(HBpz_3Fe)_2OH(OAc)_2]ClO_4$ (V).[22] The EXAFS contributions of the 2-Å Fe–O and 2.1-Å Fe–N bonds could not be resolved; therefore identical A, ΔE, and σ^2 values were used for 2O and 3N atoms, and r_{Fe-N} was constrained to be r_{Fe-O} + 0.12 Å. The 0.12 Å difference was determined from crystal structures of II–V. This approach allowed determination of the presence of a short Fe–O bond and the average Fe–X bond length for the other ligands in the above-mentioned compounds as well as in $[Fe_2L(OH)(H_2O)_2]$ and $[Fe_4L_2(O)_2(OH)_2]^{4-}$,[23] complexes with structures that differ somewhat from the hemerythrin active site. The addition of shell 2A improved the fit but did not significantly affect the Fe–Fe distances in Table I. The errors in r (EXAFS vs. crystallography) for the seven model complexes have standard deviations of 0.015, 0.02, and 0.03 for shells 1, 2B, and 3, respectively.

Table I lists structural parameters obtained for metHrN_3, native B_2 and its radical-free form, and $[(HBpz_3Fe)_2O(OAc)_2]$. The metHrN_3 parameters agree with values derived from recent crystallographic[9] and EXAFS[12,24] analyses of metHr complexes. No significant differences are observed between native and radical-free B_2. The iron centers in B_2 possess a short Fe–O bond (1.78 Å) as in metHrN_3, confirming the presence of the oxo bridge indicated by magnetic susceptibility[6] and resonance Raman[8] measurements. The Fe–Fe distance is found to be 3.2 Å and the

(17) Abbreviations used: acac, 2,4-pentanedione; $HBpz_3$, hydrotris(pyrazolyl)borate; OAc, acetate; tacn, 1,4,7-triazacyclononane; L, *N,N'*-(2-hydroxy-5-methyl-1,3-xylylene)bis[*N*-(carboxymethyl)glycine].

(18) Iball, J.; Morgan, C. H. *Acta Crystallogr.* **1967**, *23*, 239–244.
(19) Armstrong, W. H.; Spool, A.; Papaefthymiou, G. C.; Frankel, R. B.; Lippard, S. J. *J. Am. Chem. Soc.* **1984**, *106*, 3653–3667.
(20) Armstrong, W. H.; Lippard, S. J. *J. Am. Chem. Soc.* **1985**, *107*, 3730–3731.
(21) Wieghardt, K.; Pohl, K.; Gebert, W. *Angew. Chem., Intl. Ed. Engl.* **1983**, *22*, 727.
(22) Armstrong, W. H.; Lippard, S. J. *J. Am. Chem. Soc.* **1984**, *106*, 4632–4633.
(23) Murch, B. P.; Boyle, P. D.; Que, L., Jr. *J. Am. Chem. Soc.* **1985**, *107*, 6725–6729.
(24) Co, M. S. Ph. D. Thesis, Stanford University, Stanford, CA, 1983. Hendrickson, W. A.; Co, M. S.; Smith, J. L.; Hodgson, K. O.; Klippenstein, G. L. *Proc. Natl. Acad. Sci. U.S.A.* **1982**, *79*, 6255–6259.

Fe–O–Fe angle is calculated to be 127°. The close agreement of these values among B_2, metHrN$_3$, and the model compound suggests that B_2 also has the μ-oxobis(μ-carboxylato)diiron core; spectral similarities among these have also led others to suggest this common structure.[8,19] Histidine is probably coordinated to the cluster in B_2 as indicated by the low Z scatterers at 4.3 Å in the EXAFS spectrum and solvent-exchangeable features at 24 ppm in the NMR spectrum.[25] Shell 1B of B_2 is, however, 0.07 Å shorter than that of metHrN$_3$; this suggests that at least one of the terminal nitrogenous ligands of each iron of metHrN$_3$ is replaced by an oxyanion ligand, i.e., hydroxide, phenolate, or carboxylate, in B_2. Fe–O(anion) bonds are typically 0.1–0.2 Å shorter than Fe–N bonds in high-spin ferric complexes.[19-23] Differences in the coordination environments of B_2 and metHrN$_3$ are also suggested by a solvent-nonexchangeable feature at 19 ppm in the NMR spectrum of B_2[25] which is absent in metHrN$_3$.[26] Raman studies indicate the presence of coordinated hydroxide.[27] The replacement of a histidine at 2.15 Å with a hydroxide at 1.95 Å per iron would decrease the average bond length for shell 1B by 0.04 Å.

In summary, our EXAFS results indicate that the iron cluster in subunit B_2 of ribonucleotide reductase shares common structural units with that in metHrN$_3$; however, the two sites are not identical.

Acknowledgment. This work was supported by the National Science Foundation (DMB-8314935, L.Q.) and the National Institutes of Health (GM-29595, J. S.). The Cornell High Energy Synchrotron Source is supported by NSF Grant DMR-8412465. R.C.S. is grateful for postdoctoral fellowship support from the NIH and the American Cancer Society. L.Q. is an Alfred P. Sloan Research Fellow and an NIH Research Career Development Awardee. S.P.S. acknowledges a predoctoral fellowship from the NSF. J.S. is an H.I. Romnes Fellow from the University of Wisconsin—Madison and an NIH Research Career Development Awardee. We thank Profs. S.J. Lippard and Karl Wieghardt for their generous gifts of III and IV, respectively.

(25) Sahlin, M.; Ehrenberg, A.; Graslund, A.; Sjöberg, B.-M. *J. Biol. Chem.* **1986**, *261*, 2778–2780.
(26) Maroney, M. J.; Lauffer, R. B.; Que, L., Jr.; Kurtz, D. M., Jr. *J. Am. Chem. Soc.* **1984**, *106*, 6445–6446.
(27) Loehr, T. M.; Sanders-Loehr, J.; Sjöberg, B.-M., personal communication.

Isobacteriochlorophyll *b* Analogues from Photoreduction of Metallochlorins

Kevin M. Smith,* Daniel J. Simpson, and Kevin M. Snow

Department of Chemistry, University of California Davis, California 95616

Received May 19, 1986

In light of the recent interest in the chemistry and synthesis of isobacteriochlorins, we have reinvestigated the photoreduction of zinc(II) methyl pyropheophorbide *a* (ZnPPheo, **1**) previously reported by Seely.[1] It has been known for some time that ascorbic acid photoreduction of zinc(II) phylloerythrin methyl ester with diazabicyclo[2.2.2]octane (DABCO) as a catalyst gives the thermodynamically least stable *cis*-pheophorbide (dihydroporphyrin).[2] However, no detailed structural or stereochemical information on further photoreduction of such dihydroporphyrins to isobacteriochlorins (tetrahydroporphyrins) appears in the literature. Seely proposed that when photoreduced with ascorbic acid and DABCO, [magnesium(II) or] zinc(II) PPheo (**1**) gives (magnesium or) zinc methyl 2-ethylisobacteriochlorin (ZnEIBC, **2**). This conclusion was primarily based on interpretation of absorption spectra of the EIBCs and of their oxidation products.[1] Herein we show that the initial photoreduction proceeds by way of simple cis reduction of a macrocyclic double bond to give a vinylisobacteriochlorin (VIBC) and that the double bond then migrates toward the macrocycle to give the first synthetic entry to a macrocyclic product bearing an ethylidene system similar to that found in bacteriochlorophylls (BChl) *b* and *g* and in the phycobilin chromophores. Demonstration of this fundamental chemistry suggests that the thermodynamically favorable sequence of macrocycle reduction, followed by "inward" vinyl double bond migration, is a viable alternative to the accepted direct vinyl reduction followed by "outward" macrocyclic double-bond migration to ethylidene in the biosynthesis of the BChl *b* and *g*, and the phycobilins.

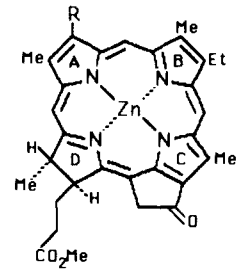

1 R = CH=CH$_2$
7 R = Et

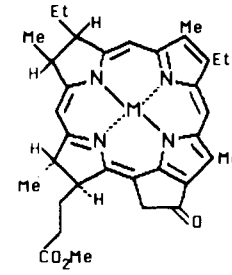

2 M = Zn
8 M = 2H
9 M = Ni
} EIBC

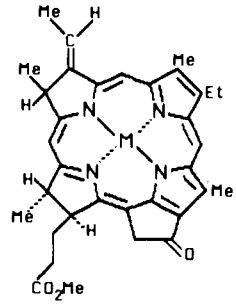

3 M = Zn
5 M = 2H
} EdIBC

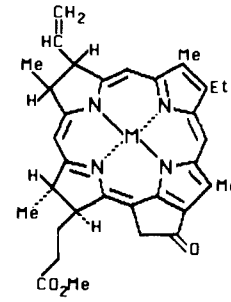

4 M = Zn
6 M = 2H
} VIBC

Seely's experiments were, by and large, carried out in spectrophotometry cuvettes. However, we have found that 100 mg of ZnPPheo (**1**) can be conveniently photoreduced in 8–10% ethanol in pyridine containing ascorbic acid and DABCO. Irradiation (fluorescent tubes, white light) of this mixture overnight produced 55 mg of reduced product. The visible absorption spectrum was consistent with that previously reported[1] for the zinc complex with a long-wavelength absorption maximum in pyridine at 626 nm and a shoulder (byproduct) around 608 nm (Figure 1A).

The proton NMR spectrum of the 626-nm product (in $CHCl_3$ and pyridine-d_5) was inconsistent with the expected product, ZnEIBC (**2**), but the meso proton chemical shifts (8.38, 7.56, 6.56 ppm) confirmed that ring A had been reduced. On the basis of extensive decoupling and nuclear Overhauser enhancement (NOE) studies, we conclude that the product is the zinc(II) ethylideneisobacteriochlorin (ZnEdIBC, **3**) rather than ZnEIBC (**2**). The network of NOE connectivities and chemical shifts in ring A is given in Figure 2. These same studies confirmed that, as with ring C in bacteriochlorophyll *b*,[3] the ethylidene group has the *E* configuration.[4]

(1) Seely, G. R. *J. Am. Chem. Soc.* **1966**, *88*, 3417–3422.
(2) Wolf, H.; Scheer, H. *Justus Liebigs Ann. Chem.* **1973**, 1710–1740, 1740–1749. Wolf, H.; Scheer, H. *Tetrahedron Lett.* **1972**, 1111–1114, 1115–1118.
(3) Scheer, H.; Svec, W. A.; Cope, B. T.; Studier, M. H.; Scott, R. G.; Katz, J. J. *J. Am. Chem. Soc.* **1974**, *96*, 3714–3716.

0002-7863/86/1508-6834$01.50/0